# Range study of Eu implanted into Si channeling directions: Evidence for the $Z_1$ effect

G. de M. Azevedo, M. Behar, and P. L. Grande
*Instituto de Física da Universidade Federal do Rio Grande do Sul, Avenida Bento Gonçalves 9500, 91501-970, Porto Alegre, Brazil*

I. Borges, Jr.*
*Departamento de Físico-Química, Instituto de Química, Universidade Federal Fluminense, Brazil*
(Received 3 May 2000; published 10 January 2001)

Eu ions have been implanted along the Si ⟨100⟩, ⟨111⟩, and ⟨110⟩ directions at 623 K with energies ranging from 15 keV to 50 keV. The depth profiles have been measured using Rutherford backscattering spectroscopy (RBS). A signature of the nuclear $Z_1$ effect, namely, the enhanced ion range found for some projectiles penetrating into amorphous Si, has been observed under channeling conditions for the Eu ions, through the appearance of extended long tails. The results have been compared to MARLOWE calculations using different interatomic potentials in order to simulate the mechanism responsible for the $Z_1$ effect. In addition, *ab initio* calculations for the Eu-Si interatomic potential have been performed in order to investigate the origin of the nuclear $Z_1$ effect. These calculations show that the formation of quasimolecules at very low energies is responsible for the enhanced ion range.

DOI: 10.1103/PhysRevB.63.064101 PACS number(s): 61.85.+p, 34.50.Bw, 68.55.Ln, 34.20.Cf

## I. INTRODUCTION

The interatomic potential is a very important issue concerning the physics of penetrating particles at relatively low incident energies. In connection with slowing down statistics, it determines several basic physical properties (stopping power, scattering cross section, damage, etc.) that have been studied for many years in materials science. The current strategy to compute the interatomic potential in atomic collisions in solids is the use of a common screening function and a corresponding screening length. This unifies the treatment for all ion-target combinations and results in the similarity concept, largely investigated by Firsov[1,2] and Lindhard, Scharff, and Schiøtt (LSS). The use of a unique interatomic screening function has recently been put forth by Ziegler and Biersack through the introduction of the Ziegler, Biersack, and Littmark (ZBL) potential,[3] grounded on free-electron gas (FEG) calculations.[4] In general, remarkable agreement has been found between the results of range measurements and the ZBL predictions. However, some important differences have been found, among them, the so-called $Z_1$ effect or $Z_1$ oscillations. It was first found by Besenbacher and co-workers[5,6] and Kalbitzer and co-workers[7–9] and systematically studied by Fichtner and co-workers.[10,11] This effect appears when some heavy ions are implanted in amorphous Si. The measured projected range of the implanted ions is strongly underestimated by the theoretical predictions, the disagreement being a function of the implantation energy, which is very large at energies below 20 keV and vanishes at $E \geqslant 70$ keV. The $Z_1$ oscillations cannot be reproduced by using FEG calculations for each specific ion-target combination. They have been attributed to deformation of the electronic clouds during the projectile-target collision. For simple gas systems[6] *ab initio* calculations indicate the formation of a quasimolecule. However, for solids and heavy projectiles, no direct calculations have been done so far. In what follows we will use the term $Z_1$ effect not for the effect as a function of (neighboring) atomic numbers, but in a more general way, for the systematic difference between the experimental data and theoretical predictions based on a common interatomic screening function and corresponding screening length (such as the ZBL interatomic potential) found at low implantation energies.

Since the $Z_1$ effect comes from collisions at large impact parameters it is natural to address the question of its influence for axial channeling implantations. In this case, the ions are focused and the ion flux has a maximum in the middle of the channel. Then, a reduced energy loss due to the possible formation of a quasimolecule will give rise to larger ion ranges than those predicted by standard calculations.

In this work we have investigated the $Z_1$ effect under axial channeling conditions. In previous range studies[11] it has been observed that Eu implanted into amorphous Si has $Z_1$ effect characteristics whereas Bi implanted ions do not. Lately, it was also observed that even under channeling conditions the Bi range profile at low energies[12] does not present the $Z_1$ effect. Then, in view of the above considerations, it is interesting to ask whether and how the $Z_1$ effect appears for Eu implantations under channeling conditions. For this purpose, we have implanted Eu along Si ⟨100⟩, ⟨110⟩, and ⟨111⟩ directions at energies from 15 up to 50 keV, and determined the corresponding depth profiles by using the Rutherford backscattering (RBS) and RBS/channeling techniques. The implantations were performed at 623 K in order to avoid sizable damage on the Si substrate and consequently dechanneling during the implantation process. It will be shown that the measured range profiles of Eu ions along Si main directions display pronounced tails that are not reproduced by standard range theories. However, *ab initio* calculations of the interatomic potential using pseudopotentials for Eu colliding on Si atoms can reproduce the measured profiles for all channeling and also for random directions. In Sec. II the experimental procedure for high-temperature implantations and depth profile analysis is described. The binary collision program MARLOWE used to simulate the channeled depth profiles is also described in Sec. II. The experimental

 

results are found in Sec. III and discussed in Sec. IV in connection with theoretical simulations and *ab initio* calculations of the interatomic potential.

## II. EXPERIMENTAL AND THEORETICAL PROCEDURES

### A. Experiment

The Eu ions were implanted into Si $\langle 100 \rangle$ and Si $\langle 111 \rangle$ samples. The implantations along the $\langle 110 \rangle$ direction were performed with $\langle 100 \rangle$ samples, with a tilt angle of 45° to the sample's normal relative to beam direction. Before each implantation, the samples were cleaned and etched to remove the native oxide on the film (and other impurities on the surface) by using 10% HF acid. Immediately after, the samples were mounted on a three-axis goniometer of 0.005° precision. The evacuation of the implantation/RBS chamber started at once, yielding a final vacuum of the order of $10^{-7}$ Torr. The Si wafers were initially aligned along the desired channeling direction using an 800 keV $\alpha$-particle beam. The $\alpha$ particles were detected by a surface Si(Li) barrier detector placed at 165° with respect to the beam direction. The overall resolution of the detecting system was about 12 keV and the angular divergence of the $\alpha$ beam better than 0.03°. After the alignment the sample holder was heated to 623 K. Subsequently, the alignment of the sample was checked, in order to rule out possible effect due to dilatation of the goniometer. In the next step, the Eu implantation was performed.

The implantation of a heavy ion like Eu into Si crystal presents a basic experimental difficulty: it produces defects on the sample, even for very low implanted fluences. For this reason, Eu implantations were performed at 623 K. At this temperature, the dynamical annealing minimizes the damage produced by the ion implantation process.

In order to find the best implantation conditions we have determined, for each implantation energy, the maximum fluence that does not introduce sizable damage on the Si substrate at 623 K. For this purpose, we have implanted, with increasing Eu fluences, the $\langle 100 \rangle$ aligned Si substrate. Subsequently, we performed channeling experiments in order to determine the minimum backscattering yield $\chi_{min}$ immediately behind the Si surface peak. This procedure was followed for each Eu implantation energy. In all cases the implantation current density was of the order of 20 nA/cm$^2$.

For 30 keV Eu (at 623 K) up to a fluence of $\Phi = 1.5 \times 10^{14}$ at./cm$^2$ we did not observe any difference between the as-implanted and the virgin samples (the $\chi_{min}$ was about 4%). However, when the implantation fluence was raised to $3 \times 10^{14}$ at./cm$^2$ $\chi_{min}$ increased to 8%, indicating the formation of sizable damage in the Si substrate despite the high temperature of implantation. This tendency was more evident when the Eu fluence was increased and for $\Phi = 8 \times 10^{14}$ at./cm$^2$, where the implanted region was completely damaged ($\chi_{min} = 100\%$). For this energy we estimated that $\Phi = 1 \times 10^{14}$ at./cm$^2$ was an adequate fluence to be implanted without introducing a sizable damage in the substrate. The same procedure was followed for all implantation energies. The implantation energies varied between 15 and 50 keV and were performed in channeling direction at the three $\langle 100 \rangle$, $\langle 110 \rangle$, and $\langle 111 \rangle$ main Si axes.

The Eu as-implanted samples were analyzed both at channeling and random directions. In the latter case the samples were measured at a tilted geometry with the beam impinging at $40° - 50°$ to the sample's normal. Consequently, we improved our depth resolution down to 100 Å . The energy to depth conversion was performed using the He stopping powers from Ref. 13 for the random case and the data from Ref. 14 for the channeling measurements. The main error in the conversion procedure is due to uncertainties in the stopping power of the particles, estimated to be of the order of 5%.[13,14] On the other hand, the errors in the range measurements, estimated from the stability of the Si edge in several measurements, turned out to be better than 1.5 nm. It should be stressed that special care was taken in order to avoid pile-up effects when the samples were analyzed. For this purpose a very low (less than 10 nA) He current was used for the Rutherford backscattering under channeling conditions (RBS/Ch) experiments. In addition, an electronic pile-up rejection system was employed.

### B. Theoretical predictions

The depth profile measurements were compared with the binary collision code MARLOWE by Robinson and Torrens.[15] It is a comprehensive computer program that has been developed for the simulation of atomic displacement in a variety of crystalline solids using the binary-collision approximation to determine the particle trajectories. The atomic scattering is governed by a screened potential (Moliere,[16] ZBL,[3] etc.). These potentials are spherically symmetric and thus no solid-state effects are taken into account. However, these effects may come into play only for very large impact parameters where the valence-electron density integrated along the ion path cannot be considered as uniform. This, nevertheless, may be possible only for the widest channel of Si ($\langle 110 \rangle$). The target atoms are distributed about their lattice positions according to a Gaussian distribution due to the thermal vibrations, the amplitude being taken from the Debye-Waller model.[17] The possible effect of spatial correlation between neighbor atoms is not taken into account in the simulations because this effect is of minor importance.[18] The inelastic energy loss can be separated into local and nonlocal contributions. The program provides the positions of the implanted ions both for crystals as well as for amorphous targets. More recently the program has been improved by taking into account temporal aspects of binary collisions.[21] This last version was used in the present work.

## III. EXPERIMENTAL RESULTS

As mentioned above, in order to study the $Z_1$ effect under axial channeling conditions, we performed implantations along the Si $\langle 100 \rangle$, $\langle 111 \rangle$, and $\langle 110 \rangle$ channeling directions for different incident energies. In Figs. 1–3 the depth profiles of implanted Eu along the $\langle 100 \rangle$, $\langle 111 \rangle$, and $\langle 110 \rangle$ channeling directions are shown for energies between 15 and 50 keV. All the range profiles show similar features: they have a

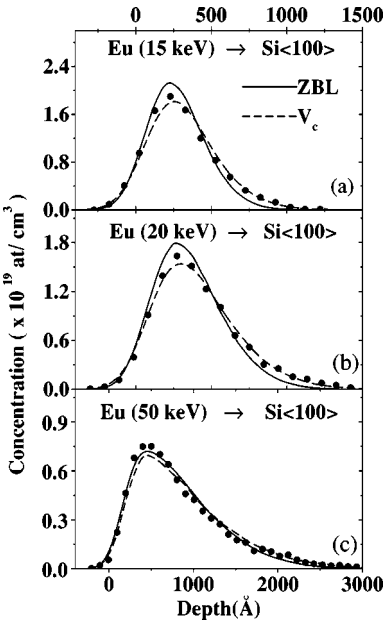


FIG. 1. Experimental data for implantations along Si ⟨100⟩ direction, for three implantation energies (full circles). Top axis for (a) and (b) and bottom axis for (c). The solid lines correspond to MARLOWE calculations with the ZBL potential and $\Theta_D = 490$ K (Ref. 12). The dashed lines correspond to MARLOWE calculations with the potential proposed in Eq. (1). In both cases, the electronic stopping is described by the Oen and Robinson model, normalized to the ZBL stopping cross section.

deep maximum and much broader distributions than those observed in amorphous Si. In addition to the experimental data, the theoretical predictions by the Monte Carlo MARLOWE program are represented by solid and dashed lines. The MARLOWE calculations were convoluted with the resolution of the electronic system in order to be compared with the experimental data. As input to the MARLOWE program we have used the ZBL interatomic potential, a modification thereof, and $\Theta_D = 490$ K as the Debye temperature. As shown in previous works,[12,19,20] this value describes the thermal vibrations of Si properly. The choice of the electronic stopping power has been shown to be of minor importance.

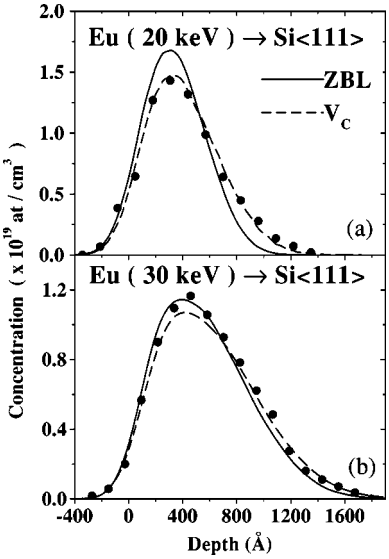


FIG. 2. Experimental data for implantations along Si ⟨111⟩ direction. See caption of Fig. 1 for further details.

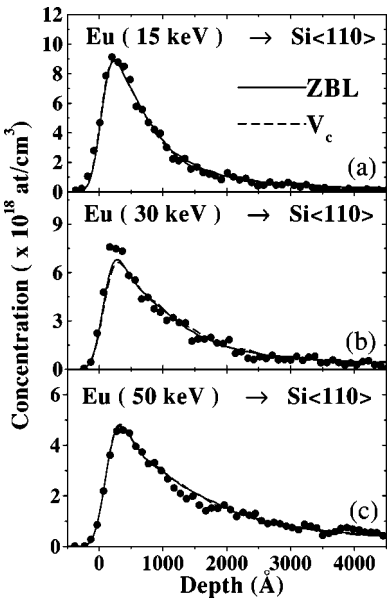


FIG. 3. Experimental data for implantations along Si ⟨110⟩ direction. See caption of Fig. 1 for further details.

An inspection of Figs. 1 and 2 shows that although the maximum of the range profile is well reproduced by the simulations, the experimental data have longer tails deep inside the target. This effect indicates that the energy loss of the well-channeled ions is overestimated by the MARLOWE standard simulation. In a previous work,[12] we implanted Bi along the Si ⟨100⟩ direction under the same conditions, in the same energy range (20–40 keV), and following a similar experimental procedure. These results were compared to MARLOWE simulations and excellent agreement was observed. In particular, the Bi concentration tails were very well reproduced by the calculations. Therefore, the appearance of the Eu longer tails, not reproduced by the simulations using the ZBL potential, can be considered to be the manifestation of the $Z_1$ effect under channeling conditions.

In principle, it could be questioned if the extended tails are spurious, originating from Eu thermal diffusion due to the high-temperature implantation, radiation-enhanced diffusion (RED), or from pile-up effects during RBS analysis. The RED mechanism can be ruled out because it would appear for all studied projectile energies and the extended tails are observed only for low energies. It should be stressed that in some few cases we have modified the Eu implantation fluence without observing any changes in the depth profile tails. Concerning the Eu diffusion mechanism, we have performed Eu diffusion experiments by doing 623 K implantations followed by thermal annealing at the same temperature for 30 min (which corresponds to the Eu implantation time). In addition, some annealings were performed for longer periods of time at the same temperature. In all cases no significant Eu diffusion was detected, the estimated upper limit for

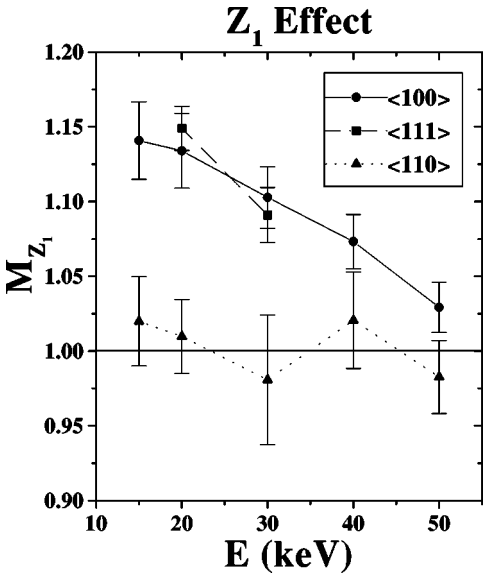


FIG. 4. Magnitude of the nuclear $Z_1$ effect ($M_{Z_1}$) defined in terms of the full widths at one fifth of the maximum (FWFM) of the Eu depth profiles.

the diffusion coefficient being $1\times10^{-20}$ m$^2$ s$^{-1}$. Thus diffusion mechanism cannot account for the observed extended tails. Concerning the pile-up effects it could be mentioned that in addition to the analysis in random direction, the range profiles have also been determined in channeling directions. Under these conditions pile-up effects are strongly reduced. Finally, it should be emphasized that we have not observed differences between the Eu-RBS spectra taken under random or channeling directions.

Another feature shown in Figs. 1–3 that corroborates the manifestation of the $Z_1$ effect is the dependence of the extended long tails on the projectile energy. This dependence was already observed when the Eu implantations were performed in random directions and it has been taken as a signature of the $Z_1$ effect.[10,11] We can quantify this effect by taking the width of the range distribution at 1/5 of the maximum (FWFM). The ratio $M_{Z_1}$ between the FWFM for the experimental data and the FWFM from the MARLOWE calculations is displayed in Fig. 4, as a function of the projectile energy, for the three channeling directions. As can be observed from this figure, the effect is largest for the lowest implantation energy and decreases with increasing ion energies, disappearing at 50 keV. Furthermore, the effect is very similar for the Si $\langle100\rangle$ and $\langle111\rangle$ channeling directions. These two channels have about the same cross section, although the geometry is quite different, yielding almost the same maximum impact parameter in an ion-target collision (1.4 Å for the $\langle100\rangle$ and 1.5 Å for the $\langle111\rangle$ direction). Since the $Z_1$ effect is related to small energy transfers in ion-solid collisions, we would expect larger effects for implantations along the widest channel of Si, namely, the $\langle110\rangle$ direction. However, as can be observed in Fig. 2, the range distribution of Eu implanted along the $\langle110\rangle$ direction, at energies ranging from 15 keV to 50 keV, observed as well as in Fig. 4, the FWFM as a function of the Eu energy, there is no difference, within the experimental errors, between the experimental Si $\langle110\rangle$ data and the MARLOWE simulation. It is also pointed out that along this direction the Eu penetrates depths about 25 times larger than those in random directions.

## IV. DISCUSSIONS

### A. Channeling depth profiles

As was mentioned in the Introduction the $Z_1$ effect was first observed by Besenbacher *et al.*[5] and Kalbitzer and co-workers[8,7] and further characterized by Fichtner and co-workers.[10,11] It was found that Au and Eu, among other ions implanted into amorphous Si, give rise to projected ranges larger than standard theoretical predictions. The effect was quite noticeable at very low implantation energies and disappears completely for $E\geqslant70$ keV. The present results for the $\langle100\rangle$ and $\langle111\rangle$ directions show the same characteristics, but mainly regarding the tail distributions. They are not reproduced by MARLOWE calculations based on the ZBL interatomic potential, the simulated distributions being shallower than the experimental ones. The difference decreases with increasing implantation energy, reaching good agreement for $E\sim50$ keV. This behavior differs from what was observed when Bi ions were implanted into Si $\langle100\rangle$ direction at different energies.[12] In this case the MARLOWE calculations, using the same input parameters as in the present case, have reproduced quite well the experimental results for the all implantation energies.

For random materials, a semiphenomenological approach to describe the $Z_1$ effect has been successfully applied to a wide variety of projectiles implanted into amorphous Si.[11] This procedure was based on the reduction of the nuclear energy transfer by cutting the interatomic potential at the sum of the ionic radii.[11] In order to reproduce the experimental channeling range profiles of Eu we have followed the same procedure. Thus, MARLOWE simulations were carried out, cutting the potential energy (the ZBL potential) at distances where a quasimolecule could be formed, about the sum of ionic radii of Eu and Si. The results of the simulations, although reproducing the experimental findings for amorphous Si—see Refs. 10 and 11, are in complete disagreement with the channeling experimental data. In fact, the introduction of a cutoff in the interatomic potential not only reduces the stopping power of the ions, but also leads to an enhancement of the dechanneling. Figure 5 displays the projectile scattering angle in the laboratory system as a function of the impact parameter for a collision of 20 keV Eu on Si. For an impact parameter of about the cutoff distance ($\sim11a_{ZBL}$, where $a_{ZBL}$ is the ZBL screening length for the Eu-Si pair) a rainbow scattering is observed, namely, a divergent differential scattering cross section at $\theta\sim0.6°$, which strongly enhances the dechanneling probability. Therefore, the interatomic potential should be modified in a different way in order to avoid artificial dechanneling processes at low-energy implantation.

Here we implement a nonabrupt reduction of the interatomic potential energy by multiplying the ZBL interatomic potential by a Fermi-Dirac function as

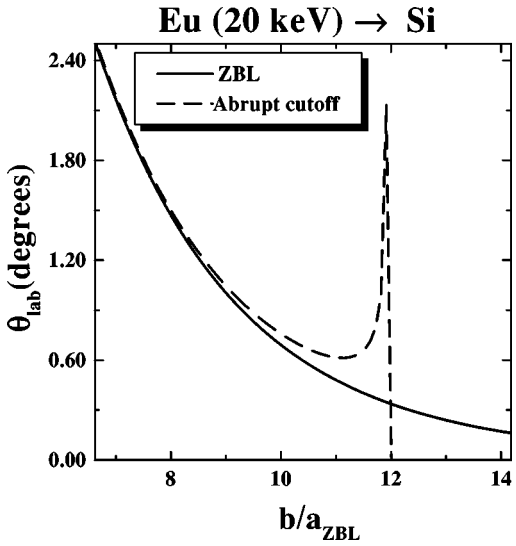


FIG. 5. Scattering angle (in the laboratory frame of reference) as a function of the impact parameter in units of $a_{ZBL}$ ($a_{ZBL}=0.106$ Å), for the ZBL potential (solid line) and for the ZBL potential with an abrupt cutoff (dashed line) as proposed in Ref. 11.

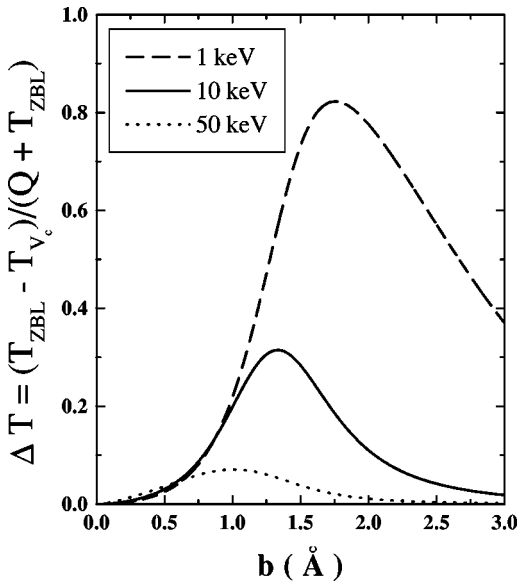


FIG. 6. The magnitude $\Delta T$ of the nuclear $Z_1$ effect, as a function of the impact parameter, for three projectiles energies 1, 10, and 50 keV. See text for further details.

$$V_c(r)=V_{ZBL}\frac{1}{1+\exp[(r-R_c)/\Delta R_c]} \tag{1}$$

where $R_c$ is a distance corresponding to the sum of ionic radii of the projectile and target, and $\Delta$ is a parameter related to the width above which the potential energy is negligible. Thus, for finite values of $\Delta$ this potential does not have any abrupt cut at $R_c$. In fact, by choosing $\Delta=0.2$, we have found a rather good agreement between the MARLOWE simulations and all channeling experimental data (see dashed lines in Figs. 3–5) for all implantation energies and directions as well as for the depth profiles obtained in amorphous silicon—not shown here. The same holds true even for the depth distributions along the Si $\langle 110\rangle$, for which the original agreement was already good.

We are now in position to investigate why the $Z_1$ effect is negligible for the widest channel in Si, namely, the $\langle 110\rangle$ one. As mentioned in Sec. III, the electronic energy loss plays a very minor role in the determination of the implantation profile for channeling Eu in the present energy range. However, due to the strong reduction of the nuclear energy transfer at distances about the sum of the ionic radii, the electronic energy loss may dominate over the nuclear one at very large impact parameters. Then, in the case of a very open channel, the long tails are dominated by the electronic energy loss and the $Z_1$ effect is much less pronounced.

The $Z_1$ effect can be quantified by taking the difference $\Delta T(b)$ between the nuclear energy transfer calculated with the ZBL interatomic potential and the one with the potential $V_c$ from Eq. (1). In Fig. 6 $\Delta T(b)$ normalized to the total energy transfer $T_{total}(b)$ is displayed as a function of the impact parameter for three projectile energies. Here we have used $T_{total}=T_{ZBL}+Q(b)$, where $Q(b)$ is the electronic energy loss according to the Oen and Robinson formula.[22] An inspection of this figure shows, first, as expected, that the effect of reducing the interatomic potential is larger for low-energy collisions and disappears for projectile energies higher than 50 keV. Second, the effect has a maximum for collisions with a given impact parameter. This behavior is a consequence of the dominance of the electronic energy loss over nuclear one. It means that for very open channels, such as the Si $\langle 110\rangle$, the $Z_1$ effect in the nuclear energy loss is overshadowed by the electronic stopping power.

### B. *Ab initio* interatomic potential for Eu-Si

The interatomic potential from Eq. (1) is able to reproduce all channeling depth distributions describing, in this way, the extended long tails observed for Eu implantation along Si $\langle 100\rangle$ and $\langle 111\rangle$. However, this potential comes from a best fit procedure with a single parameter. Then, in order to verify that the observed extended tails really come from a reduction of the potential energy between the projectile and target due to a formation of a quasimolecule, we have performed *ab initio* calculations of the interatomic potential for the Eu-Si pair. The GAUSSIAN94 program was used throughout.[23]

Although ground-state calculations involving two first and/or second row atoms are common in computational chemistry, this is not so for heavier elements. Quantum chemistry calculations involving lanthanide atoms have only recently received greater attention due to their intrinsic chemical interest, theoretical challenge, and the appearance of more powerful computer resources.

The ground-state electronic configuration of the two atoms are Si:$[\mathrm{Ne}]3s^2 3p^2$ ($^3P$) and $[\mathrm{Xe}]4f^7,6s^2$ ($^8F$), where $[X]$ represents the electronic configuration of the noble gas $X$. The spin multiplicity is $(2S+1)$, $S$ being the spin quantum number, and equals 3 for Si and 8 for the Eu. The Eu atom, like some lanthanides and some actinides, has a high spin multiplicity because its ground state is stabilized by having

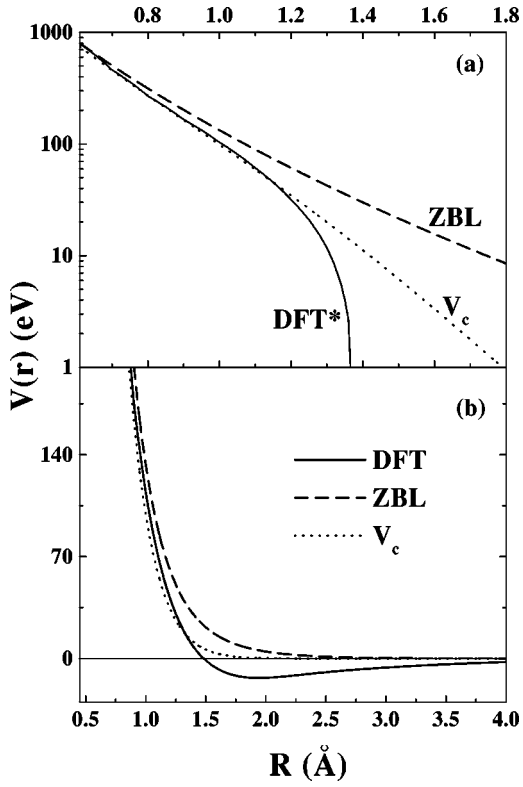


FIG. 7. (a) ZBL potential (dashed line) compared to the DFT* (DFT potential subtracted by 10 eV) (solid line) and to the potential $V_c$ (dotted line) proposed in Eq. (1). (b) DFT potential shown in detail. As it can be seen, the DFT potential is attractive for $R \geqslant 1.4$ Å.

the greatest possible exchange energy, the value of which value is only nonzero for electrons having parallel spins.

As the purpose of the *ab initio* calculations was to check if the Si and Eu atoms, assumed to be in their ground states, would have a stabilization energy not provoked by an artificial binding due to spin pairing (the usual way that bonds are formed in stable molecules), we computed the *ab initio* energies assuming that each atom preserved its original spin multiplicity. Therefore, we have performed the calculations using a total spin multiplicity of 10 for the Eu-Si system. Further details of the present calculation are presented in the Appendix.

Figure 7 shows the results of the *ab initio* calculations [density functional theory (DFT)] for the Eu-Si interatomic potential. In order to better compare the DFT with the $V_c$ and the ZBL potentials, Fig. 7(a) displays the DFT potential energy subtracted by 10 eV (see DFT*). In fact, this does not change the dynamics of the collisions, but requires a redefinition of the energy in the center of mass frame.

For interatomic distances smaller than 0.6 Å the DFT potential is equal to the ZBL potential. For larger distances up to 1.2 Å , the calculated potential is identical to the $V_c$ and for $r > 1.4$ Å the DFT potential is attractive, with a minimum near $r = 2$ Å. Then, the *ab initio* calculation shows the formation of an stable quasimolecule, even with the nonallowance of spin pairing.

Given the results of the DFT calculations, it would be highly desirable to introduce the DFT potential in MARLOWE and compare its predictions to our experimental data. However, the introduction in MARLOWE of a potential with an atractive region is not a trivial task. In fact, the implementation of the binary collision approximation in our version of MARLOWE (version 13c) deals with strictly repulsive potentials. Nevertheless, it is possible to draw some interesting conclusions by comparing the DFT potential with the $V_c$ potential from Eq. (1). For example, for the interatomic distances above $r > 1.4$ Å for which the potential $V_c$ differs from the DFT calculations, the interaction energy is of the order of 10 eV. In the laboratory frame of reference, this corresponds to the potential energy at the distance of closest approach in a head-on collision between an Eu ion with 50 eV of kinetic energy and a Si atom. An Eu with such a low energy has a range representing only a tiny contribution to its total range. In other words, the $V_c$ potential is identical to the *ab initio potential* in the region of interatomic distances relevant to the determination of the implantation depth profiles. In this way, one can foresee that the introduction of the DFT potential in MARLOWE will not change substantially the predictions of the $V_c$ potential.

The above discussion gives strong theoretical support to the phenomenological potential that we have suggested in Eq. (1). The introduction of the $V_c$ potential in MARLOWE is able to reproduce all the available experimental data on Eu implantations on Si (both for random and channeling implantations). Moreover, ab inito calculations of the interatomic potential have also been performed for the Bi-Si system. In this case the obtained potential is purely repulsive, that is, no quasimolecule formation is observed. This feature is in agreement with the absence of $Z_1$ effect for this system for random[10,11] as well as for channeling implantations.[12] Thus, we find strong evidence that the $Z_1$ effect has its origin in the formation of quasimolecules during low-energy collisions.

## V. CONCLUSIONS

In the present work we have investigated the depth profiles of Eu ions implanted under channeling conditions along the Si $\langle 100 \rangle$, $\langle 110 \rangle$, and $\langle 111 \rangle$ directions in the 15 to 50 keV energy interval. The experimental results were compared with the predictions of MARLOWE, a simulation program that requires, among other input parameters, an interatomic potential to describe the Eu-Si binary collision. The Eu depth profiles along the Si $\langle 100 \rangle$ and $\langle 111 \rangle$ directions show long tails deep in the Si bulk not reproduced by the MARLOWE simulations. The theoretical-experimental disagreement is maximum for the lowest implantation energies and decreases with increasing energy, achieving quite good agreement for the highest energy (50 keV). This behavior is a signature of the nuclear $Z_1$ effect already observed for the same ion-target combination but for amorphous Si. We have also observed the absence of this effect for the $\langle 110 \rangle$ direction. In fact since this channel is the widest in Si, the electronic stopping plays an important role and is dominant over the nuclear one, hiding in this way the $Z_1$ effect. In order to reproduce our experimental results we have introduced a

smooth cutoff in the ZBL potential at an interatomic distance corresponding to the sum of the ionic radii of Eu and Si. Following this procedure we were able to reproduce not only all the channeling data but also the previous ones obtained for Eu implanted in amorphous Si. It should be pointed out that this agreement was obtained with only one free parameter in the interatomic potential, a parameter that has the same value for all simulations. In order to get an inside view on the underlying physics involved with this semiempirical potential we have performed *ab initio* calculations for the Eu-Si interatomic potential based on density functional theory. The results have shown that the formation of Eu-Si quasimolecules is responsible for the nuclear $Z_1$ effect for low-energy ion-target collisions. This argument was previously advanced but never proved in a conclusive way as done in the present case.

## ACKNOWLEDGMENTS

This work was partially supported by the Brazilian agencies Conselho Nacional de Desenvolvimento Científico e Tecnológico (CNPq) and Financiadora de Estudos e Projetos (FINEP). We thank Andre G. H. Barbosa for his help on the early stages of the *ab initio* calculations.

## APPENDIX

The present *ab initio* calculations of the interatomic potential employed the Gaussian basis set known as SBKJC.[24,25] The core electrons were assumed to be frozen, described by an effective core potential (ECP) for each atom. Therefore, the core electrons screen the Coulomb field from the nuclei, this physical effect being described by an ECP. The Gaussian basis set had 8 electrons as the Si core[24] and 46 electrons for Eu,[25] both cores described by ECP's. The remaining electronic shells were described by atom centered Gaussian functions. Both basis sets included relativistic effects in the description of their ECP's, known to be especially important for heavy atoms such as the lanthanides.

The Hartree-Fock approximation does not give a balanced description of potential energy curves over the whole range of internuclear distances $R$. The reason is that the interaction between the electrons are treated in an average way. Therefore, it is necessary to go beyond the Hartree-Fock approximation to describe the correlation of the electrons' movement. We accomplished this through density functional theory (DFT) calculations based on the self-consistent Kohn-Sham procedure.[26,27]

The DFT theory is based on the electronic density distribution $n(r)$. Its starting point is writing an energy functional dependent on the electronic distribuition,

$$E[n(r)] \equiv \int v(r)n(r)dr + \langle \Psi[n(r)]|T+U|\Psi[n(r)]\rangle, \tag{A1}$$

where $v(r)$ is an arbitrary external potential, $U$ is the interelectronic Coulomb repulsion between the electrons, $T$ is the kinetic energy of the electrons, and $\Psi$ is the full $N$-particle ground-state wave function. From this equation it is possible to obtain an upper bound for the ground-state energy. By making suitable approximations to the second term in the above equation, $F[n(r)]=\langle \Psi[n(r)]|T+U|\Psi[n(r)]\rangle$, it is possible to rederive the Thomas-Fermi equations and its refinements.[26,27] We may extract from $F[n(r)]$ its largest and elementary contributions,

$$F[n(r)] = T_s[n(r)] + \frac{1}{2}\int \frac{n(r)n(r')}{|r-r'|}drdr' + E_{exc}[n(r)], \tag{A2}$$

where $T_s[n(r)]$ is the kinetic energy of a *noninteracting* system with density $n(r)$, and the next term is the classical expression for the interaction energy. The $E_{exc}$ term is the so-called exchange correlation energy and it is defined by the above equation.

It is then possible to transform the Euler-Lagrange equation associated with the stationarity of $E_{exc}$ into a new set of self-consistent equations, the so-called Kohn-Sham equations.[26,27] If in principle an exact expression for $E_{exc}$ could be obtained, the Kohn-Sham equations would be exact. However, there is no exact expression for $E_{exc}$, and the various variants of the DFT models are distinct one from another according to the form of the function $E_{exc}$. In the present work we used a correlation generalized gradient approximation[26,27] for $E_{exc}$ known as B3LYP, as it uses Becke's three-parameter exchange functional[28] (B3) with the Lee-Yang-Parr correlation functional[29] (LYP). This form of $E_{exc}$ has been used very much in the literature, and has given good results for a great variety of molecular systems. In order to obtain the interatomic potential, we have also to add the contribution of the Eu and Si core electrons. This was performed by using the free-electron gas approximation FEG.[4]

*Present address: Departamento de Química, Universidade de Coimbra, Coimbra P-3049, Portugal.

[1] O. B. Firsov, Zh. Éksp. Teor. Fiz. **32**, 1464 (1957) [Sov. Phys. JETP **5**, 1192 (1957)]; **33**, 696 (1958) [**6**, 534 (1958)].
[2] J. Lindhard, M. Scharff, and H. E. Schiøtt, Mat. Fys. Medd. K. Dan. Vidensk. Selsk. **33**, 1 (1963).
[3] J. F. Ziegler, J. P. Biersack, and U. Littmark, *The Stopping and Range of Ions in Solids* (Pergamon, New York, 1985).
[4] R. G. Gordon and Y. S. Kim, J. Chem. Phys. **56**, 3122 (1972).
[5] F. Besenbacher, J. Bøttiger, T. Laursen, P. Loftager, and W. Möller, Nucl. Instrum. Methods **170**, 183 (1980).
[6] P. Loftager, F. Besenbacher, O. S. Jensen, and V. S. Sørensen, Phys. Rev. A **20**, 1443 (1979).
[7] K. Izsak, J. Berthold, and S. Kalbitzer, Nucl. Instrum. Methods Phys. Res. B **15**, 34 (1986).
[8] J. Berthold and S. Kalbitzer, Nucl. Instrum. Methods **209/210**, 13 (1983).
[9] S. Kalbitzer and H. Oetzmann, Radiat. Eff. **47**, 57 (1980).
[10] P. F. P. Fichtner, M. Behar, C. A. Olivieri, R. P. Livi, J. P. de Souza, F. C. Zawislak, D. Fink, and J. P. Biersack, Nucl. In-

strum. Methods Phys. Res. B **15**, 58 (1986).
[11] M. Behar, P. F. P. Fichtner, P. L. Grande, and F. C. Zawislak, Mater. Sci. Eng., R. **15**, 1 (1995).
[12] G. de M. Azevedo, J. C. Martini, M. Behar, and P. L. Grande, Nucl. Instrum. Methods Phys. Res. B **149**, 301 (1999).
[13] D. Niemann, P. Oberschachtsiek, S. Kalbitzer, and H. P. Zeindl, Nucl. Instrum. Methods Phys. Res. B **80/81**, 37 (1993); D. Niemann, G. Kognac, and S. Kalbitzer, Nucl. Instrum. Methods Phys. Res. B **118**, 11 (1996).
[14] J. H. R. dos Santos, P. L. Grande, H. Boudinov, M. Behar, R. Stoll, Chr. Klatt, and S. Kalbitzer, Nucl. Instrum. Methods Phys. Res. B **106**, 5 (1995).
[15] M. T. Robinson and I. M. Torrens, Phys. Rev. B **9**, 5008 (1974).
[16] G. Moliere, Z. Naturforsch. A **2**, 133 (1947).
[17] W. Eckstein, *Computer Simulation of Ion-Solid Interactions* (Springer-Verlag, Berlin, 1991), and references therein.
[18] S. Alliney, F. Malaguti, and E. Verondini, Nucl. Instrum. Methods Phys. Res. B **28**, 10 (1987).
[19] A. Dygo, P. J. M. Smoulders, and D. O. Boerma, Nucl. Instrum. Methods Phys. Res. B **64**, 701 (1992).
[20] G. Hobler, A. Simionescu, L. Palmetshofer, F. Jahnel, R. von Criegern, C. Tian, and G. Stingeder, J. Vac. Sci. Technol. B **14**, 272 (1996).
[21] M. T. Robinson, Nucl. Instrum. Methods Phys. Res. B **40**, 10 717 (1989).
[22] O. S. Oen and M. T. Robinson, Nucl. Instrum. Methods **132**, 647 (1976).
[23] M. J. Frish, G. W. Trucks, H. B. Schlegel, P. M. W Gill, B. G. Johnson, M. A. Robb, J. R. Cheeseman, T. Keith, G. A. Petersson, J. A. Montgomery, K. Raghavachari, M. A. Al-Laham, V. G. Zakrzewski, J. V. Ortiz, J. B. Foresman, J. Cioslowski, B. B. Stefanov, A. Nanayakkara, M. Challacombe, C. Y. Peng, P. Y. Ayala, W. Chen, M. W. Wong, J. L. Andres, E. S. Replogle, R. Gomperts, R. L. Martin D. J. Fox, J. S. Binkley, D. J. Defrees, J. Baker, J. P. Stewart, M. Head-Gordon, C. Gonzalez, and J. A. Pople, GAUSSIAN94, Revision E.1 (Gaussian, Inc., Pittsburgh, PA, 1995).
[24] W. J. Stevens, H. Basch, and M. Krauss, J. Chem. Phys. **81**, 6026 (1984).
[25] T. R. Cundari and W. J. Stevens, J. Chem. Phys. **98**, 5555 (1993).
[26] R. G. Parr and W. Yang, *Density Functional Theory of Atoms and Molecules* (Oxford University Press, New York, 1989).
[27] W. Kohn, A. D. Becke, and R. G. Parr, J. Chem. Phys. **100**, 12 974 (1996).
[28] A. D. Becke, J. Chem. Phys. **98**, 5648 (1993).
[29] C. Lee, W. Yang, and R. G. Parr, Phys. Rev. B **37**, 785 (1988).